Assessing the accuracy of screened range-separated hybrids for bulk properties of semiconductors

Stefan A. Seidl ⓘ, Bernhard Kretz ⓘ, Christian Gehrmann ⓘ, and David A. Egger ⓘ*
Department of Physics, Technical University of Munich, 85748 Garching, Germany

Density functional theory calculations using well-established semilocal and hybrid functionals are typically accurate for structural properties of semiconductors, but they often fail to quantitatively describe electronic-structure and optical properties of these materials. An improvement to conventional hybrid functionals is the class of screened range-separated hybrid (SRSH) functionals. In the SRSH approach, the range-separation parameter is used to empirically fit the band gap of the semiconductor, which was shown to lead to highly accurate predictions of electronic-structure and optical properties. Here we assess the accuracy of the SRSH approach for computing other important bulk properties of seven prototypical semiconductors, including lattice constants and phonon dispersion relations. Our SRSH results are compared to data from semilocal (PBE) and hybrid (HSE) functional calculations as well as to experimental data from the literature. We find that SRSH can compete with the high accuracy provided by the two well-established functionals PBE and HSE for computing bulk properties of semiconductors. Furthermore, similarly to the case of the HSE functional, the SRSH method yields phonon dispersion relations of semiconductors that tend to be more accurate than those calculated with PBE. The SRSH approach thus provides a consistently accurate framework for calculations of semiconductor bulk properties.

I. INTRODUCTION

Theoretical calculations of static and dynamic bulk properties are key to a microscopic understanding of semiconductors and their properties. For example, theoretical predictions related to static quantities, such as the lattice constant, are required when new semiconductors and their properties are explored in the absence of experimental data and guidance. In regard to dynamic properties, calculations of vibrational spectroscopy (e.g., infrared or Raman activities), of heat- as well as electrical transport, need computations of lattice dynamics as an input. The most common approach to compute static and dynamic bulk properties for semiconductors is density functional theory (DFT) using (semi-) local exchange-correlation (XC) functionals, such as LDA [1] or PBE [2]. Hybrid functionals that include a fraction of Fock exchange have been popular in quantum chemistry for decades, and their application to computing properties of bulk semiconductors is well established too.

Of particular relevance for semiconductors are DFT calculations with so-called screened hybrid functionals [3], in which a range separation of the Coulomb operator is used to screen long-range interactions in the bulk material. Popular screened hybrids, such as the HSE functional [4,5], have been extensively tested for semiconductors [6–9]. Indeed, screened hybrid functionals do improve some of the well-known deficiencies of (semi-) local DFT, e.g., the HSE functional often provides more realistic electronic band structures and gaps than PBE [5,10]. At the same time, screened hybrids cannot be expected to perform accurately in all cases, which for semi-

conducting systems has been shown by, e.g., Jain *et al.* [11]. Still, an appealing aspect of screened hybrid functionals is that in addition to improved electronic-structure predictions, they were shown to provide accurate descriptions of lattice dynamics as well [12,13]. For example, it was demonstrated that HSE yields phonon dispersion relations of semiconductors that tend to be more accurate than those calculated with PBE [12].

A relatively recent development for solid-state calculations of semiconductors are so-called screened range-separated hybrid functionals (SRSH), in which a range separation is performed akin to the conventional screened hybrid functionals [14]. As in conventional screened hybrid functionals, in SRSH the mixing of Fock and semilocal exchange is varied depending on the distance of electrons in the system [14]. Importantly however, with its functional form SRSH can be tuned so that the correctly screened exchange interaction for a bulk material is retrieved asymptotically, i.e., $\frac{1}{\epsilon r}$ for $r \to \infty$, where ϵ is the dielectric constant of the system [14,15]. A recent study has proposed to tune the range-separation parameter in the SRSH approach to the *GW* band gap at the Γ point [16]. It has been shown that the SRSH functional tuned in this way allows for highly accurate predictions of electronic structure and optical-absorption properties of semiconductors within DFT and linear response time-dependent DFT (TD-DFT) [16,17], respectively. Furthermore, once the SRSH parameter is tuned for a given material, it can be used to reliably predict other properties. Recent examples include charge-transition levels [18] that are often challenging for DFT [19] and optical-absorption spectra of semiconductors [16,20].

In this work our main focus is on the applicability of SRSH to predict structural and lattice-dynamical properties of inorganic semiconductors. The motivation for our study

---

*david.egger@tum.de

is that from a formal perspective, it would be appealing if SRSH not only delivered accurate quantities related to the electronic structure of a given semiconductor, but also quantities related to total energies and respective derivatives. From a practical perspective, it is interesting to assess whether the superior performance of SRSH for electronic-structure and optical properties comes at a cost of reduced accuracy for other bulk properties of semiconductors. Previous work in the context of gas-phase molecules has indeed shown that the related class of optimally tuned RSH functionals not only yields highly accurate electronic properties [21,22], but also ground-state molecular geometries and vibrational frequencies [23] in addition to excited-state potential energy surfaces [24]. Indeed, a consistently accurate approach for both *electronic-structure and total-energy quantities* of semiconductors will be particularly appealing for calculations that inherently require both, such as the computation of electron-phonon couplings that are key in theories of electrical transport in semiconductors.

Therefore, in this article SRSH is used to calculate lattice-dynamical as well as other closely related bulk properties of semiconductors. Specifically, we compute equilibrium lattice constants, bulk moduli, atomization energies, and phonon dispersion relations for a set of seven semiconductors, for which the tuning of the range-separation parameter has been reported recently [16]. Our SRSH results are compared to experimental data as well as to calculations of the often used PBE and HSE functional. We find that SRSH agrees similarly well to experiments as the well-established and fairly accurate HSE and PBE functionals for the obtained bulk and phonon properties, and conclude that the superior performance of SRSH for electronic-structure and optical properties does not impede its accuracy for other bulk properties of semiconductors.

II. METHODOLOGY

A. Benchmark systems

To assess the accuracy of the SRSH functional for bulk semiconductors, we performed calculations on the following prototypical systems: AlAs, AlP, AlSb, GaAs, GaP, InP, and Si. The reasons for choosing these materials are that reference data from DFT calculations as well as experiments are readily available in the literature, and that furthermore high-level *GW* data were reported for them recently [16,25].

B. DFT calculations

We performed our DFT calculations using the Vienna *ab initio* simulation package (VASP) [26] applying a plane-wave basis set and the projector-augmented wave (PAW) method [27]. Apart from the valence electrons, we included semicore d states for Ga and In in our calculations.

Plane-wave energy cutoffs and k-point grids were converged separately for each system using the experimental lattice constant, until the change in the total energy was below 2 meV per atom using the PBE functional [2]. The resulting cut-off energies subsequently used for our calculations are reported in Table I. For the sampling of k points, we employed Γ-centered Monkhorst-Pack grids with either $8 \times 8 \times 8$ k points (AlAs, AlP, AlSb, InP) or $9 \times 9 \times 9$ k points (GaAs,

TABLE I. Plane-wave energy cutoffs used to calculate equilibrium lattice constants, bulk moduli, as well as atomization energies (E_{cut}) and phonon band structures ($E_{\text{cut}}^{\text{ph}}$).

Name	E_{cut} (eV)	$E_{\text{cut}}^{\text{ph}}$ (eV)
AlAs	220	220
AlP	245	245
AlSb	190	240
GaAs	280	380
GaP	300	350
InP	255	355
Si	270	270

GaP, Si). For the supercell calculations (see Sec. II F), we reduced the k points to a grid of $2 \times 2 \times 2$.

C. The SRSH functional

In the SRSH functional, the Coulomb potential is split in the following way [22,28,29]:

$$\frac{1}{r} = \frac{\alpha + \beta \ \text{erf}(\gamma r)}{r} + \frac{1 - [\alpha + \beta \ \text{erf}(\gamma r)]}{r}. \quad (1)$$

The first term on the right-hand side is treated with Fock exchange (EXX), and the second term with exchange from the generalized gradient approximation (GGA). With this, one obtains the following for the exchange-correlation energy:

$$E_{\text{XC}}^{\text{SRSH}} = \alpha E_{\text{X,SR}}^{\text{EXX}} + (1 - \alpha) E_{\text{X,SR}}^{\text{GGA}} + (\alpha + \beta) E_{\text{X,LR}}^{\text{EXX}}$$
$$+ [1 - (\alpha + \beta)] E_{\text{X,LR}}^{\text{GGA}} + E_{\text{C}}^{\text{GGA}}. \quad (2)$$

The subscript X indicates exchange and C correlation, SR denotes short range, and LR denotes long range. The parameters α and β determine the amount of Fock exchange in the short and long range, and γ is the range-separation parameter.

Here we apply SRSH parameters reported in previous work [16]. Specifically, we use $\alpha = 0.25$ for all materials, and set $\alpha + \beta = \frac{1}{\epsilon}$, with ϵ being the dielectric constant of the material, which ensures the correct asymptotic decay of the exchange-correlation potential. The dielectric constants have been obtained in previous work with HSE calculations [16]. Finally, the range-separation parameter γ was also chosen for each semiconductor according to Ref. [16], which fitted γ so that the GW band gap at the Γ point was reproduced by SRSH. Band gaps calculated with SRSH, HSE as well as PBE can be found in the Supplemental Material (SM) [30]. The SRSH parameters used in our calculations are summarized in Table II.

We compare the SRSH results to data from experiment and from calculations using two popular functionals for semiconductors, namely the GGA functional PBE [2] and the screened hybrid HSE [4,5]. While the two hybrid functionals have been obtained in an empirical fashion (see Refs. [4,5] for HSE and above for SRSH), the PBE functional has been parametrized nonempirically to reproduce certain properties of the exact density functional [2]. Note that PBE as well as HSE can be obtained from the SRSH functional by setting α and β to zero for the former, and β to $-\alpha$ and γ to 0.20 Å^{-1} for the latter, in Eq. (2). For a comparison of the computational

TABLE II. SRSH parameters used in this work for the seven studied semiconductors, see text for details.

Name	$\epsilon_\infty^{\text{theory}}$	α	β	γ (Å^{-1})
AlAs	8.2	0.25	-0.13	1.25
AlP	7.3	0.25	-0.11	0.80
AlSb	9.8	0.25	-0.15	0.63
GaAs	10.5	0.25	-0.15	2.50
GaP	8.9	0.25	-0.14	1.15
InP	8.9	0.25	-0.14	1.30
Si	11.3	0.25	-0.16	0.62

times associated with the three functionals see Table IX in the SM [30].

D. Lattice constant and bulk modulus

We computed the equilibrium lattice constant of each material with the different functionals. For this purpose, the total energy E for unit-cell volumes V between 91% and 109% (in steps of 3%) of the experimental volume was calculated. We then used the Birch-Murnaghan equation of state [31–33] to fit $E(V)$ as

$$E(V) = E_0 + \frac{B_0 V}{B_0'}\left(\frac{(V_0/V)^{B_0'}}{B_0' - 1} + 1\right) - \frac{V_0 B_0}{B_0' - 1}. \quad (3)$$

In this equation E_0 is the free energy at equilibrium volume V_0, and B_0 and B_0' are the bulk modulus and its derivative with respect to pressure, respectively.

E. Atomization energy

We calculated the atomization energies, E_{AE}, for the different materials according to

$$E_{\text{AE}}(M) = \frac{1}{N}\left[\sum_{\text{atoms}} E_0(X) - E_0(M)\right]. \quad (4)$$

Here $E_0(M)$ is the total energy of the semiconductor M, $E_0(X)$ is the energy of a single constituent atom X in the supercell of a given material (see Sec. II F), and N the number of atoms in the supercell.

F. Phonon dispersion relations

The finite-difference method as implemented in Phonopy [34] was employed to compute phonon band structures using $4 \times 4 \times 4$ supercells. For certain materials, the plane-wave cut-off energy had to be notably increased (see Table I) in order to avoid numerical issues in the calculations, such as imaginary frequencies at the Γ point. Nonanalytical term corrections as developed by Pick *et al.* [35] with an interpolation to finite q points as described in Refs. [36,37] were included for all systems except Si.

III. RESULTS

A. Lattice constants and bulk moduli

The lattice constants of the seven semiconductors computed with PBE, HSE, and SRSH are shown together with

experimental data in Table III. Generally, we find that all three functionals provide lattice constants in very good agreement with room temperature experimental values. But note that despite the fact that they were computed at 0 K, they still somewhat overestimate the finite-temperature experimental results. For the SRSH functional, the mean absolute deviation (MAD) from the experimental lattice constants across all materials is 0.04 Å and the maximum deviation (MD) is 0.07 Å. Thus, it lies between the accuracy of HSE (MAD 0.02 Å, MD 0.03 Å) and PBE (MAD 0.07 Å, MD 0.10 Å). The HSE lattice constants are generally shorter than the PBE ones, a trend which also has been found in previous studies [49–51]. It is important to note that SRSH-computed lattice constants do not deviate by more than 0.04 Å from the HSE values, indicating that the former can maintain the accuracy of the latter for calculating lattice constants of semiconductors.

Table IV shows the bulk moduli for the different semiconductors calculated with the three functionals as well as a range of experimental values from literature. The MADs and MDs compared to the arithmetic mean of experiment are 10 (MAD) and 16 GPa (MD) for PBE, 4 (MAD) and 10 GPa (MD) for SRSH, and 1 (MAD) and 4 GPa (MD) for HSE. Thus, as is the case for the lattice constants, the SRSH functional can compete with the accuracy of HSE also for calculations of bulk moduli. In agreement with previous work [7], we find here that the overestimation of lattice constants by PBE correlates with an underestimation of bulk moduli. A similar but significantly weaker trend can be observed for the SRSH functional, which slightly underestimates the bulk moduli of all materials except AlP. For most of the semiconductors, the accurate lattice constants provided by HSE coincide with deviations of HSE bulk moduli to experimental data that are smaller than the range of experimental values.

B. Atomization energies

We calculated the atomization energies for the seven semiconductors with the three functionals, see Table V. Among the three functionals, PBE gives atomization energies closest to experimental data, while HSE and SRSH values are slightly farther away. Specifically, the MADs compared to experiment are 0.10 (PBE), 0.11 (HSE), and 0.14 eV (SRSH). Hence, while the calculations with the three functionals underestimate experimental atomization energies, they all still perform reasonably well. It is, however, noteworthy that zero-point corrections, which are not considered here, would lower DFT atomization energies further [7]. Moreover, the accuracy of all three functionals for this quantity strongly depends on the material under investigation, leading to deviations of our DFT atomization energies with respect to experiments between -0.4% and -9.0%.

C. Phonon dispersion relations

Phonon band structures of all semiconductors were calculated in two ways: First, with the equilibrium lattice constant computed with the respective functional for each material as reported above, and second following another common practice (see, e.g., Ref. [59]), that is to use the experimental lattice constant reported in the literature. Generally, we find that the

TABLE III. Comparison of the lattice constant a obtained with the PBE, HSE, and SRSH functional to room temperature experimental data for all studied systems [38].

	PBE		HSE		SRSH		Expt.
Name	a (Å)	Deviation (%)	a (Å)	Deviation (%)	a (Å)	Deviation (%)	a (Å)
AlAs	5.74	1.4	5.68	0.4	5.70	0.7	5.66
AlP	5.51	0.9	5.47	0.2	5.48	0.4	5.46
AlSb	6.24	1.6	6.15	0.2	6.18	0.7	6.14
GaAs	5.75	1.8	5.68	0.5	5.72	1.2	5.65
GaP	5.51	1.1	5.46	0.2	5.48	0.6	5.45
InP	5.96	1.5	5.90	0.5	5.93	1.0	5.87
Si	5.47	0.7	5.44	0.2	5.45	0.4	5.43
MAD(%)		1.3		0.3		0.7	

accuracy of the different functionals for phonon calculations depends on how accurate the respective theoretical lattice constants are. Specifically, PBE generally underestimates the phonon frequencies compared to experiment and compared to HSE and SRSH, in line with our finding that PBE also underestimates the lattice constants (cf. Table III). Between HSE and SRSH, no clear trend regarding the accuracy of the phonon frequencies can be observed. When, on the other hand, the experimental lattice constant is used for phonon calculations, the three functionals give similar phonon frequencies. This assessment about the accuracy of the calculated phonon frequencies is supported when their specific values are compared to experimental data that is available for high-symmetry points (see Tables II to VIII of the SM [30]).

We now report further details and show the phonon dispersion relations for GaAs and Si in Figs. 1 and 2. We choose to show results for these two systems because deviations in their theoretical lattice constant with respect to experiment are largest and smallest, respectively. Thus, we expect the spread of the phonon frequencies computed with the three functionals for these two systems to be largest and smallest as well. The phonon dispersion relations for the remaining semiconductors can be found in the SM [30].

In the case of the GaAs phonon frequencies calculated with the theoretical lattice constant (see left panel of Fig. 1), we observe the following trend: a more accurate theoretical lattice constant leads to phonon frequencies that are closer to experiment, which holds for acoustic and optical phonon branches. Therefore, HSE provides the most accurate phonon frequencies in this case, followed by SRSH and PBE. Furthermore, since the calculations with the three functionals overestimate the lattice constant, the phonon frequencies are generally underestimated.

When we use the experimental lattice constant to compute the phonon dispersion relation (see right panel of Fig. 1), we see that the spread among results from the three functionals is reduced: for the LO phonon energy at Γ the spread is lowered from 0.7 to 0.2 THz when the experimental instead of theoretical lattice constant is used, i.e., all functionals provide relatively similar and very accurate phonon frequencies. A more detailed analysis shows that the accuracy depends on whether acoustic or optical phonons are considered. For acoustic branches, HSE results appear closest to experimental data, but especially SRSH and also the PBE results are quite close as well. For optical branches we find that all three functionals give similarly accurate results, except around the Γ point, where HSE slightly overestimates, PBE slightly underestimates, and SRSH provides the most accurate frequencies.

For Si phonon dispersions calculated with the theoretical lattice constant (see left panel of Fig. 2), all three functionals give similarly accurate results for the acoustic phonon frequencies. For optical phonons, SRSH provides the most accurate frequencies compared to experiment, while PBE slightly under- and HSE slightly overestimates them. Thus, trends in the accuracy of the Si phonon dispersion relation do not follow the one found for lattice constants, since the spread

TABLE IV. Comparison of the bulk modulus B obtained with the PBE, HSE, and SRSH functional to room temperature experimental data for all studied systems.

	PBE		HSE		SRSH		Expt.
Name	B (GPa)	Deviation (%)	B (GPa)	Deviation (%)	B (GPa)	Deviation (%)	B (GPa)
AlAs	67	−11	76	+1	72	−5	74–77 [39,40]
AlP	81	−7	89	+2	90	+3	86–88 [41,42]
AlSb	49	−13	58	+3	55	−3	55–58 [42–44]
GaAs	60	−21	72	−5	66	−13	75–76 [45,46]
GaP	78	−11	88	+1	84	−4	87–88 [40,47]
InP	62	−14	71	−1	67	−7	71–73 [40,48]
Si	89	−10	98	−1	95	−4	98–99 [40,45]
MAD(%)		12		2		5	

TABLE V. Comparison of the atomization energy E_{AE} obtained with the PBE, HSE, and SRSH functional to experimental data for all studied systems.

Name	PBE		HSE		SRSH		Expt.
	E_{AE} (eV/atom)	Deviation (%)	E_{AE} (eV/atom)	Deviation (%)	E_{AE} (eV/atom)	Deviation (%)	E_{AE} (eV/atom)
AlAs	3.73	−1.3	3.70	−2.1	3.68	−2.6	3.78 [52]
AlP	4.13	−3.1	4.10	−3.8	4.08	−4.2	4.26 [52]
AlSb	3.28	−0.9	3.28	−0.9	3.27	−1.2	3.31 [53]
GaAs	3.18	−3.9	3.16	−4.5	3.13	−5.4	3.31 [6]
GaP	3.52	−1.1	3.51	−1.4	3.47	−2.5	3.56 [52]
InP	3.16	−7.9	3.15	−8.2	3.12	−9.0	3.43 [54]
Si	4.60	−0.4	4.58	−0.9	4.56	−1.3	4.62 [55]
MAD(%)		2.7		3.1		3.8	

of the calculated lattice constants is small for Si (cf. Table III). The phonon dispersion relation calculated with experimental lattice constant (see right panel of Fig. 2) is slightly overestimated by both hybrid functionals, which give almost identical phonon frequencies. For optical branches, PBE is closest to experiment, while for acoustic branches the hybrid functionals yield more accurate frequencies. Overall, differences among PBE, HSE, and SRSH are minor in this case.

IV. DISCUSSION

For static bulk properties we found that the HSE and SRSH functional provided more accurate lattice constants and bulk moduli, while the PBE functional described atomization energies somewhat better than the two hybrid functionals. This finding is reminiscent of the known impact of the reduced density gradient in GGA functionals. Specifically, it has been shown that the strength of the reduced density gradient in GGA determines whether lattice constants or atomization energies are described more accurately by a given GGA functional [60]. A manifestation of this can be seen when comparing the accuracy of the PBE and PBEsol functional for those quantities [60]: the main difference between those two functionals is that the influence of the density gradient is weakened in PBEsol compared to PBE, leading to an improved description of lattice constants while deteriorating the accuracy for atomization energies [60]. Since in HSE and

SRSH 75% PBE exchange is used in the short range, one could argue that this may impact the influence of the PBE reduced density gradient, leading to more accurate lattice constants and less accurate atomization energies. In passing we note that for SRSH atomization energies, one could in principle tune the range-separation parameter γ for bulk and isolated atom separately. However, total energies obtained with different γ values cannot be compared and, thus, the atomization energy cannot be calculated this way [61].

For dynamic bulk properties we found that all three functionals appear to be accurate in comparison to experiment, but also that HSE and SRSH frequencies often lie somewhat closer to experiment than those obtained with PBE. In this context we note that key ingredients in phonon calculations are forces acting on displaced nuclei. Our findings suggest that the influence of the amount of exact exchange and the density gradient in the short range on these forces, and thus on the phonon frequencies, is rather small. This leads to very similar phonon dispersion relations for the three functionals, especially when these are calculated with the experimental lattice constant.

Taken together, this leaves us with an important insight: previous work showed that SRSH-calculated band-structure and optical properties are very close to GW-BSE, when a single empirical parameter was fitted such that the SRSH gap reproduces the GW gap at the Γ point [16]. We showed here that at the same time the SRSH approach can compete with
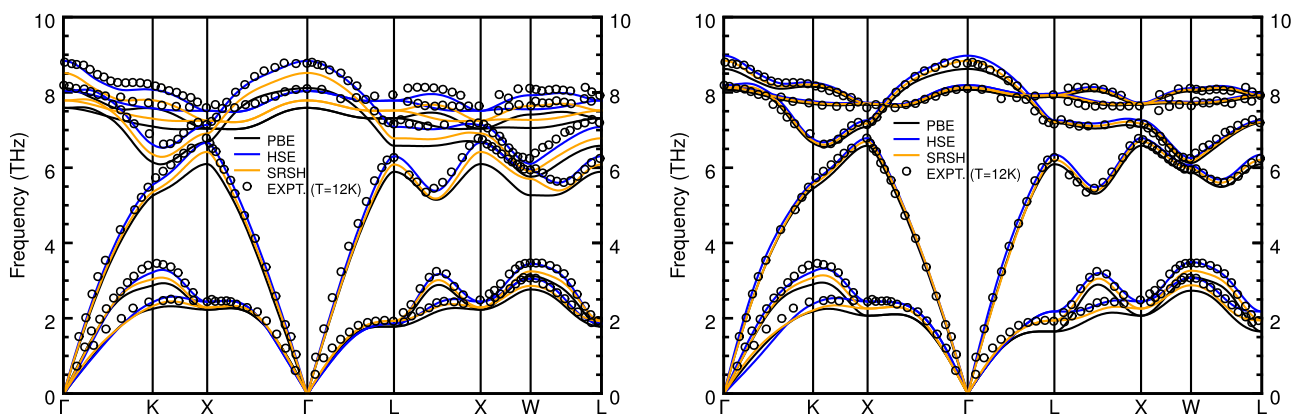

FIG. 1. Phonon dispersion relation of GaAs calculated with theoretical (left panel) and experimental (right panel) lattice constants. Experimental data have been extracted from Ref. [56].
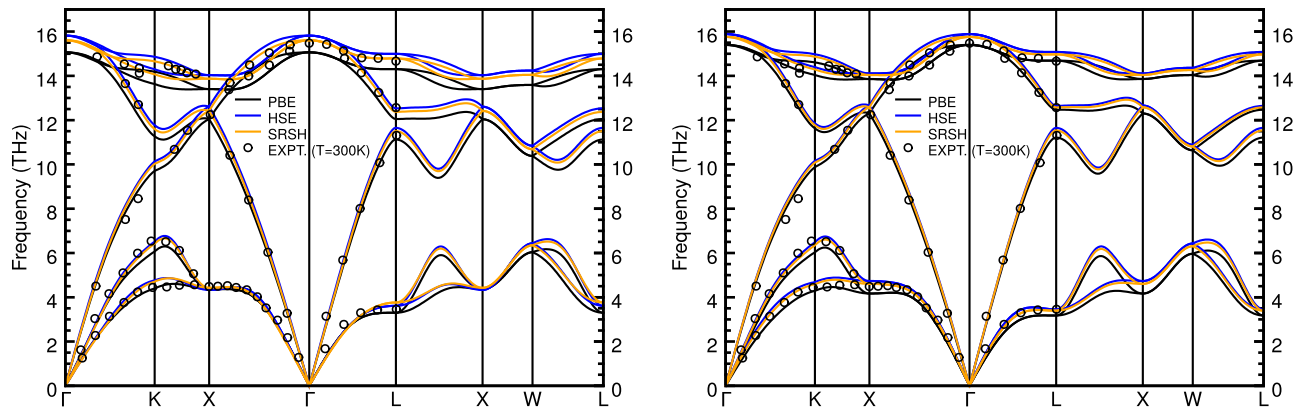
FIG. 2. Phonon dispersion relation of Si calculated with theoretical (left panel) and experimental (right panel) lattice constants. Experimental data have been extracted from Refs. [57,58].

the accuracy provided by PBE and HSE for computation of other important bulk properties of semiconductors. Moreover, especially for phonon frequencies the SRSH method outperforms the PBE functional and provides similar accuracy as the HSE functional. This means that the SRSH approach provides a consistent framework for computing bulk properties of semiconductors with high accuracy.

Besides the influence of the amount of Fock exchange on various physical quantities that was investigated and discussed here, we note that there are further effects which may play a certain role. Examples are the already mentioned zero-point corrections or the contribution from dispersive interactions, such as van der Waals interactions. In regard to the latter, it has been shown that including dispersive corrections in the XC functional lowers the lattice constant while increasing the atomization energy of semiconductors [62]. At the same time, whether including dispersive corrections provided an improvement of the theory was shown to depend on the used functional [62]. For this reason, we decided to perform our calculations without dispersive corrections allowing for an easier comparison among the three considered functionals.

V. CONCLUSION

In summary, we benchmarked the accuracy of the SRSH approach for calculating important static and dynamic bulk properties of seven prototypical semiconductors. To this end we compared SRSH results for lattice constants, bulk moduli,

atomization energies, and phonon dispersion relations to data calculated with the often used XC functionals PBE and HSE and to experimental literature values. Overall, we found that for these quantities, SRSH can compete with the accuracy provided by HSE and PBE. Our study has therefore shown that the already established high accuracy of SRSH for calculating electronic-structure and optical properties of semiconductors does not lead to a deteriorated performance for calculating other important properties of semiconductors. We conclude that SRSH provides a consistent and accurate framework for computing properties of bulk semiconductors.

[1] J. P. Perdew and A. Zunger, Self-interaction correction to density-functional approximations for many-electron systems, Phys. Rev. B **23**, 5048 (1981).

[2] J. P. Perdew, K. Burke, and M. Ernzerhof, Generalized Gradient Approximation Made Simple, Phys. Rev. Lett. **77**, 3865 (1996).

[3] B. G. Janesko, T. M. Henderson, and G. E. Scuseria, Screened hybrid density functionals for solid-state chemistry and physics, Phys. Chem. Chem. Phys. **11**, 443 (2009).

[4] J. Heyd, G. E. Scuseria, and M. Ernzerhof, Hybrid functionals based on a screened Coulomb potential, J. Chem. Phys. **118**, 8207 (2003).

[5] A. V. Krukau, O. A. Vydrov, A. F. Izmaylov, and G. E. Scuseria, Influence of the exchange screening parameter on the performance of screened hybrid functionals, J. Chem. Phys. **125**, 224106 (2006).

[6] J. Paier, M. Marsman, and G. Kresse, Why does the B3LYP hybrid functional fail for metals? J. Chem. Phys. **127**, 024103 (2007).

[7] J. Paier, M. Marsman, K. Hummer, G. Kresse, I. C. Gerber, and J. G. Ángyán, Screened hybrid density functionals applied to solids, J. Chem. Phys. **124**, 154709 (2006).

[8] M. Marsman, J. Paier, A. Stroppa, and G. Kresse, Hybrid functionals applied to extended systems, J. Phys.: Condens. Matter **20**, 064201 (2008).

[9] Y. Hinuma, A. Grüneis, G. Kresse, and F. Oba, Band alignment of semiconductors from density-functional theory and many-body perturbation theory, Phys. Rev. B **90**, 155405 (2014).

[10] J. Heyd, J. E. Peralta, G. E. Scuseria, and R. L. Martin, Energy band gaps and lattice parameters evaluated with the Heyd-Scuseria-Ernzerhof screened hybrid functional, J. Chem. Phys. **123**, 174101 (2005).

[11] M. Jain, J. R. Chelikowsky, and S. G. Louie, Reliability of Hybrid Functionals in Predicting Band Gaps, Phys. Rev. Lett. **107**, 216806 (2011).

[12] K. Hummer, J. Harl, and G. Kresse, Heyd-Scuseria-Ernzerhof hybrid functional for calculating the lattice dynamics of semiconductors, Phys. Rev. B **80**, 115205 (2009).

[13] Q. Cai, D. Scullion, A. Falin, K. Watanabe, T. Taniguchi, Y. Chen, E. J. G. Santos, and L. H. Li, Raman signature and phonon dispersion of atomically thin boron nitride, Nanoscale **9**, 3059 (2017).

[14] S. Refaely-Abramson, S. Sharifzadeh, M. Jain, R. Baer, J. B. Neaton, and L. Kronik, Gap renormalization of molecular crystals from density-functional theory, Phys. Rev. B **88**, 081204(R) (2013).

[15] L. Kronik and S. Kümmel, Dielectric screening meets optimally tuned density functionals, Adv. Mater. **30**, 1706560 (2018).

[16] D. Wing, J. B. Haber, R. Noff, B. Barker, D. A. Egger, A. Ramasubramaniam, S. G. Louie, J. B. Neaton, and L. Kronik, Comparing time-dependent density functional theory with many-body perturbation theory for semiconductors: Screened range-separated hybrids and the G W plus Bethe-Salpeter approach, Phys. Rev. Mater. **3**, 064603 (2019).

[17] S. Refaely-Abramson, M. Jain, S. Sharifzadeh, J. B. Neaton, and L. Kronik, Solid-state optical absorption from optimally tuned time-dependent range-separated hybrid density functional theory, Phys. Rev. B **92**, 081204(R) (2015).

[18] D. Wing, J. Strand, T. Durrant, A. L. Shluger, and L. Kronik, Role of long-range exact exchange in polaron charge transition levels: The case of MgO, Phys. Rev. Mater. **4**, 083808 (2020).

[19] C. Freysoldt, B. Grabowski, T. Hickel, J. Neugebauer, G. Kresse, A. Janotti, and C. G. Van de Walle, First-principles calculations for point defects in solids, Rev. Mod. Phys. **86**, 253 (2014).

[20] D. Wing, J. B. Neaton, and L. Kronik, Time-dependent density functional theory of narrow band gap semiconductors using a screened range-separated hybrid functional, Adv. Theory Simul. **3**, 2000220 (2020).

[21] T. Stein, H. Eisenberg, L. Kronik, and R. Baer, Fundamental Gaps in Finite Systems from Eigenvalues of a Generalized Kohn-Sham Method, Phys. Rev. Lett. **105**, 266802 (2010).

[22] S. Refaely-Abramson, S. Sharifzadeh, N. Govind, J. Autschbach, J. B. Neaton, R. Baer, and L. Kronik, Quasiparticle Spectra from a Nonempirical Optimally Tuned Range-Separated Hybrid Density Functional, Phys. Rev. Lett. **109**, 226405 (2012).

[23] I. Tamblyn, S. Refaely-Abramson, J. B. Neaton, and L. Kronik, Simultaneous determination of structures, vibrations, and frontier orbital energies from a self-consistent range-separated hybrid functional, J. Phys. Chem. Lett. **5**, 2734 (2014).

[24] B. Kretz and D. A. Egger, Accurate molecular geometries in complex excited-state potential energy surfaces from time-dependent density functional theory, J. Chem. Theory Comput. **17**, 357 (2021).

[25] B. D. Malone and M. L. Cohen, Quasiparticle semiconductor band structures including spin-orbit interactions, J. Phys.: Condens. Matter **25**, 105503 (2013).

[26] G. Kresse, and J. Furthmüller, Efficient iterative schemes for ab initio total-energy calculations using a plane-wave basis set, Phys. Rev. B **54**, 11169 (1996).

[27] P. E. Blöchl, Projector augmented-wave method, Phys. Rev. B **50**, 17953 (1994).

[28] T. Yanai, D. P. Tew, and N. C. Handy, A new hybrid exchange-correlation functional using the Coulomb-attenuating method (CAM-B3LYP), Chem. Phys. Lett. **393**, 51 (2004).

[29] D. Lüftner, S. Refaely-Abramson, M. Pachler, R. Resel, M. G. Ramsey, L. Kronik, and P. Puschnig, Experimental and theoretical electronic structure of quinacridone, Phys. Rev. B **90**, 075204 (2014).

[30] See Supplemental Material at http://link.aps.org/supplemental/10.1103/PhysRevMaterials.5.034602 for the remaining phonon dispersion relations of AlAs, AlP, AlSb, GaP and InP, which includes Refs. [63–68], as well as specific phonon frequencies at high-symmetry points for all semiconductors. Furthermore, the band gaps are listed for all semiconductors, as well as an example for a comparison of the computation time.

[31] F. Birch, Finite elastic strain of cubic crystals, Phys. Rev. **71**, 809 (1947).

[32] F. D. Murnaghan, The Compressibility of media under extreme pressures, Proc. Natl. Acad. Sci. USA **30**, 244 (1944).

[33] C. L. Fu and K. M. Ho, First-principles calculation of the equilibrium ground-state properties of transition metals: Applications to Nb and Mo, Phys. Rev. B **28**, 5480 (1983).

[34] A. Togo and I. Tanaka, First principles phonon calculations in materials science, Scr. Mater. **108**, 1 (2015).

[35] R. M. Pick, M. H. Cohen, and R. M. Martin, Microscopic theory of force constants in the adiabatic approximation, Phys. Rev. B **1**, 910 (1970).

[36] Y. Wang, J. J. Wang, W. Y. Wang, Z. G. Mei, S. L. Shang, L. Q. Chen, and Z. K. Liu, A mixed-space approach to first-principles calculations of phonon frequencies for polar materials, J. Phys.: Condens. Matter **22**, 202201 (2010).

[37] A. Togo, L. Chaput, and I. Tanaka, Distributions of phonon lifetimes in Brillouin zones, Phys. Rev. B **91**, 094306 (2015).

[38] W. Martienssen and H. Warlimont (Eds.), *Springer Handbook of Condensed Matter and Materials Data*, Springer Handbooks (Springer, Berlin, 2005).

[39] O. Madelung, U. Rössler, and M. Schulz (Eds.), Landolt-Börnstein Semiconductors (Springer, Berlin, 2002), Vols. 41A1b and 41A1a.

[40] O. Madelung, *Semiconductors: Data Handbook*, 3rd ed. (Springer, Berlin, 2004).

[41] P. Rodriguez-Hernandez and A. Munoz, Ab initio calculations of electronic structure and elastic constants in AlP, Semicond. Sci. Technol. **7**, 1437 (1992).

[42] S. B. Zhang and M. L. Cohen, High-pressure phases of III-V zinc-blende semiconductors, Phys. Rev. B **35**, 7604 (1987).

[43] H. Hirano, S. Uehara, A. Mori, A. Onodera, K. Takemura, O. Shimomura, Y. Akahama, and H. Kawamura, High-pressure phase transitions in AlSb, J. Phys. Chem. Solids **62**, 941 (2001).

[44] S. Ves, K. Strössner, and M. Cardona, Pressure dependence of the optical phonon frequencies and the transverse effective charge in AlSb, Solid State Commun. **57**, 483 (1986).

[45] V. N. Staroverov, G. E. Scuseria, J. Tao, and J. P. Perdew, Tests of a ladder of density functionals for bulk solids and surfaces, Phys. Rev. B **69**, 075102 (2004).

[46] H. J. McSkimin, A. Jayaraman, and P. Andreatch, Elastic moduli of GaAs at moderate pressures and the evaluation of compression to 250 kbar, J. Appl. Phys. **38**, 2362 (1967).

[47] S. Ves, K. Strössner, C. K. Kim, and M. Cardona, Dependence of the direct energy gap of GaP on hydrostatic pressure, Solid State Commun. **55**, 327 (1985).

[48] R. Trommer, H. Müller, M. Cardona, and P. Vogl, Dependence of the phonon spectrum of InP on hydrostatic pressure, Phys. Rev. B **21**, 4869 (1980).

[49] L. Schimka, J. Harl, and G. Kresse, Improved hybrid functional for solids: The HSEsol functional, J. Chem. Phys. **134**, 024116 (2011).

[50] Y.-S. Kim, K. Hummer, and G. Kresse, Accurate band structures and effective masses for InP, InAs, and InSb using hybrid functionals, Phys. Rev. B **80**, 035203 (2009).

[51] M. Schlipf, M. Betzinger, C. Friedrich, M. Ležaić, and S. Blügel, HSE hybrid functional within the FLAPW method and its application to GdN, Phys. Rev. B **84**, 125142 (2011).

[52] W. A. Harrison, *Electronic Structure and the Properties of Solids* (Dover, New York, 1980).

[53] B. Paulus, P. Fulde, and H. Stoll, Cohesive energies of cubic III-V semiconductors, Phys. Rev. B **54**, 2556 (1996).

[54] T. Soma, The electronic theory of III-V and II-VI tetrahedral compounds. I. Crystal energy and bulk modulus, J. Phys. C: Solid State Phys. **11**, 2669 (1978).

[55] M. W. Chase, *NIST-JANAF Thermochemical Tables* (AIP, Woodbury, NY, 1998).

[56] D. Strauch and B. Dorner, Phonon dispersion in GaAs, J. Phys.: Condens. Matter **2**, 1457 (1990).

[57] G. Dolling, *Inelastic Scattering of Neutrons in Solids and Liquids*, Vol. 11 (International Atomic Energy Agency, Vienna, 1963), p. 37.

[58] G. Nilsson and G. Nelin, Study of the homology between silicon and germanium by thermal-neutron spectrometry, Phys. Rev. B **6**, 3777 (1972).

[59] F. Favot and A. Dal Corso, Phonon dispersions: Performance of the generalized gradient approximation, Phys. Rev. B **60**, 11427 (1999).

[60] J. P. Perdew, A. Ruzsinszky, G. I. Csonka, O. A. Vydrov, G. E. Scuseria, L. A. Constantin, X. Zhou, and K. Burke, Restoring the Density-Gradient Expansion for Exchange in Solids and Surfaces, Phys. Rev. Lett. **100**, 136406 (2008).

[61] A. Karolewski, L. Kronik, and S. Kümmel, Using optimally tuned range separated hybrid functionals in ground-state calculations: Consequences and caveats, J. Chem. Phys. **138**, 204115 (2013).

[62] G.-X. Zhang, A. Tkatchenko, J. Paier, H. Appel, and M. Scheffler, van der Waals Interactions in Ionic and Semiconductor Solids, Phys. Rev. Lett. **107**, 245501 (2011).

[63] M. Welkowsky and R. Braunstein, Interband transitions and exciton effects in semiconductors, Phys. Rev. B **5**, 497 (1972).

[64] A. Onton, *Proceedings of the 10th International Conference on the Physics of Semiconductors* (USAEC, Oak Ridge, CA, 1970), p. 107.

[65] B. Monemar, Fundamental energy gaps of AlAs and AlP from photoluminescence excitation spectra, Phys. Rev. B **8**, 5711 (1973).

[66] D. Strauch, B. Dorner, and K. Karch, *Phonons 89*, edited by S. Hunklinger, W. Ludwig, and G. Weiss (World Scientific, Singapore 1990), p. 82.

[67] J. L. Yarnell, J. L. Warren, R. G. Wenzel, and P. J. Dean, Lattice dynamics of gallium phosphide, Neutron Inelastic Scattering, in *Proceedings of a Symposium on Neutron Inelastic Scattering*, Vol. 1 (International Atomic Energy Agency, Vienna, 1968), p. 301.

[68] P. H. Borcherds, G. F. Alfrey, A. D. B. Woods, and D. H. Saunderson, Phonon dispersion curves in indium phosphide, J. Phys. C: Solid State Phys. **8**, 2022 (1975).